

Motion Control of a Three Degrees of Freedom Helicopter

Amir Nobahar Sadeghi Nam

Abstract - This paper presents design and implement of control architectures for a three-degrees-of-freedom model helicopter. To design motion control system, active disturbance rejection control, fuzzy logic control and back stepping control architectures are designed and presented. Extended state observer technique has been studied in order to eliminate the disturbances on the dynamics. The performances measure of the control architectures are computed to compare the presented control architectures more accurately.

Index Terms — Three DOF Model Helicopter, Dynamic Model, Active Disturbance Rejection Control, Fuzzy Logic Control, Back-Stepping Control.

1 INTRODUCTION

A three degrees of freedom (3-DOF) helicopter is a simplified platform which has two propellers mounted on two front and back DC motors. It can be used to develop flight control architectures by controlling rotational speed of these two propellers. The motion control system should track the desired attitude angles of the helicopter. Based on the reference [1], designing a robust control system to control its attitude is difficult. The reasons of this problem have been mentioned, being an under-actuated system, strong coupling between pitch and travel motions, and model parametric uncertainties. In addition, since the helicopter system has a large delay constant, the PID controllers cannot guarantee good responses. On the other hand the system dynamics are nonlinear, time-varying and may be highly uncertain. The uncertainties, can be model parametric uncertainties or external disturbances.

Modeling of a 3-DOF helicopter have been investigated in literature and lots of control methods have been proposed centering on this issue, such as the widely used PID control, fuzzy logic, back stepping, sliding mode control, etc. Non-linear model of a 3-DOF Helicopter is developed in [2]. Dynamic identification model is employed to estimate the dynamic parameters of the helicopter. This identification model is based on an inverse dynamic model linear in the parameters, and is performed by the sensors data when the helicopter is following a trajectory. A software benchmark tool for a 3-DOF helicopter is proposed in [3], based on a multi-body model of the experimental setup. Then a novel reduced complexity non-linear model for the helicopter is extracted, and employing it, a feedback linearizing control law is proposed. Identification of the angular motion model parameters for a helicopter benchmark is proposed to design adaptive algorithms in [4]. The simplified model

represents the decoupled pitch motion and interrelated elevation and travel motions of the helicopter. A supervisory control architecture is designed for a 3 DOF helicopter in [5]. In this thesis a different approach which uses a real-time simulation of linearized plant dynamics with a feedback law is proposed to ensure the system's safety. Article [6], provides a comparative study on the performances of standard PID and adaptive PID controllers tested on travel angle of a 3-DOF helicopter. It is proposed that the performance of a PID controller could be improved if the PID controller is combined with adaptive element. Study [7] investigates the model of a 3-DOF laboratory helicopter, which yields highly nonlinear differential equations. Employing the model, a classic state vector feedback controller with integration of the control error is implemented. Based on the system parameters of the linearized model, a gain scheduling approach is developed using one of the degrees of freedom as scheduling parameter. Then, a flatness-based feedforward controller architecture is added for transient set point changes using linear and nonlinear inverse dynamics. Design and experimental validation of a nonlinear multi-variable predictive controller [8] has been presented for an educational 3 DOF helicopter system. The control strategy, approximate predictive control, is based on a neural network model of the nonlinear plant and its linearization in each sampling instant. A method of tracking control based on fuzzy control algorithm for elevation attitude of a 3-DOF helicopter has been introduced in [9]. Fuzzy controller is designed through the combination of expert knowledge and training data, which is used in its elevation attitude. Two robust control strategies via sliding-modes techniques is presented in [10]. First, quasi-continuous controllers are designed along with a sliding mode differentiator and then the design of classical PID controllers in combination with a second-order sliding

• Amir Nobahar Sadeghi Nam, Post-Doc. Research Fellow in Mechatronics engineering department, Atılım University, Ankara, Turkey
E-mail: amir.nobahar@gmail.com

mode observer is presented. The elevation and traveling fuzzy logic control strategy is presented in [11], which is based on the LQR (linear quadratic regulation). The characteristic of channel coupling and nonlinearity of the system have been resolved by dividing the workspace into four phases which the system has a linear behavior. These phases are considered independently and then LQR controllers are designed separately for each phase. Then fuzzy logic is used to combine all phases and stabilize the whole nonlinear system. Article [12], investigates the robust attitude control of a helicopter. The proposed robust control architecture has three parts: a nominal feed forward controller, a nominal LQR controller, and a robust compensator. Finally, in [13], an adaptive integral backstepping architecture is proposed to realize robust control of a 3-DOF helicopter. The presented control system can estimate model uncertainties online and improve the robustness of the control system.

In this paper, designing of three types of control systems for a 3-DOF helicopter are designed and presented. The helicopter motion dynamics is presented, then the design procedure of active disturbance rejection controller (ADRC), fuzzy logic controller (FLC) along with back stepping control (BSC) architecture are proposed. Ability of extended state observer (ESO) technique to eliminate the external disturbances is evaluated. To compare the behavior of designed control architectures more accurately, the performances measure of them are extracted. These techniques and contributions, reveal novelties for the motion control system design of 3-DOF helicopter in the theoretical domain.

2 THREE-DOF HELICOPTER DYNAMIC MODEL

The dynamic model of a three degrees of freedom helicopter represents its motion mathematically in some equations of motions. The governing equation of motions, have been presented in literature [1-13]. This model constitutes the basis for system analysis and control.

The schematic of such a helicopter is illustrated in figure 1. Based on parameter definition presented in the equations (1-4), the dynamic equations of motions will be as the equations (5-7). In these equations, ε , $\dot{\varepsilon}$, ρ , $\dot{\rho}$, λ , $\dot{\lambda}$ are the elevation, pitch and travel rotational angles and speeds respectively. K_f is the propeller force-thrust constant, M_f , M_b are mass of the front and back propellers assembly, M_w is the counter-weight, L_w is distance from travel axis to the counterweight, L_a is distance from travel axis to helicopter body, L_h is distance from pitch axis to each motor, and V_f , V_b are voltage inputs of the front and back motors. As it is appeared in the travel motion dynamics equation (7), this motion is controlled by the pitch motion dynamics.

$$b_1 = \frac{K_f L_a}{M_w L_w^2 + 2M_f L_a^2} \quad (1)$$

$$b_2 = \frac{K_f}{2M_f L_h} \quad (2)$$

$$b_3 = \frac{(L_w M_w - 2L_a M_f)g}{(M_w L_w^2 + 2M_f L_h^2 + 2M_f L_a^2)} \quad (3)$$

$$V_{op} = \frac{(L_w M_w - L_a M_f - L_a M_b)g}{2K_f L_a} \quad (4)$$

$$\ddot{\varepsilon} = b_1(V_f + V_b) \quad (5)$$

$$\ddot{\rho} = b_2(V_f - V_b) \quad (6)$$

$$\ddot{\lambda} = b_3 \rho \quad (7)$$

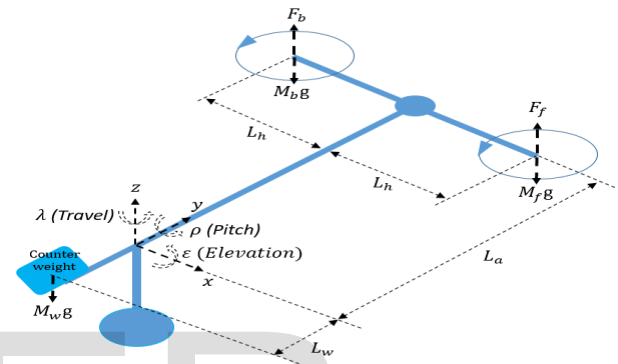


Fig. 1. Schematic of a 3-DOF Helicopter Model

3 CONTROLLER DESIGN

Three kinds of control architectures are designed to motion control of the helicopter. These controllers are active disturbance rejection controller (ADRC), fuzzy logic controller (FLC) and back stepping controller (BSC). Since there is state dependency in travel dynamics, to control its motion, a classic PID controller is employed to produce pitch reference through the travel reference in all of three control architectures.

The comparison of the designed controllers is accomplished based on the performances measures presented in [14] as illustrated in the equations (8-11). In these equations, the error signal is the difference between the reference input and measured output in elevation and pitch angles. The integral square error (ISE) represents the error energy, integral absolute error (IAE) determines the cumulative error, integral of time weighted absolute error (ITAE) displays the steady-state error, and the root mean square error (RMSE) represents the standard deviation of the errors.

$$ISE = \int e^2 dt \quad (8)$$

$$IAE = \int |e| dt \quad (9)$$

$$ITAE = \int t \cdot |e| dt \quad (10)$$

$$RMSE = \int \frac{e^2}{n} dt \tag{11}$$

3.1. Active Disturbance Rejection Controller

An active disturbance rejection controller (ADRC) consists of two main components: PD controller and Extended State Observer (ESO). This controller can successfully track the reference signal while rejecting all the parametric uncertainties and external disturbances. Schematic of an ADRC controller for the motions dynamics is displayed in figure 2.

To design this observer for elevation and pitch motions employing the equations (5-6), the dynamics of the observers should be extracted properly. Here the observer design procedure for dynamics of motions are described, based on the equations (15) and (21). In these equations, D_ϵ , D_ρ are the external disturbance effecting on the elevation and pitch dynamics respectively. The effect of the external disturbance and the model parametric uncertainties are considered as new states x_3, x_6 in these dynamics respectively. Equations (19) and (25) represents the observer dynamics. In the equations (20) and (26), $\omega_{0\epsilon}$, $\omega_{0\rho}$ are the observers bandwidths, which can be derived by bandwidth parameterization as presented in the reference [15].

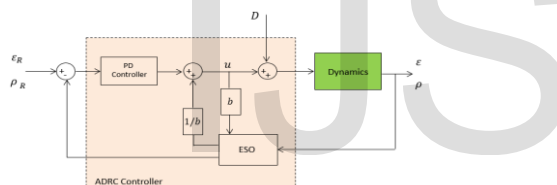


Fig. 2. Schematic of ADRC Controller

$$X = [x_1 \ x_2 \ x_3 \ x_4 \ x_5 \ x_6 \ x_7 \ x_8 \ x_9] = [\epsilon \ \dot{\epsilon} \ D_\epsilon \ \rho \ \dot{\rho} \ D_\rho \ \lambda \ \dot{\lambda} \ D_\rho + b_3\rho] \tag{12}$$

$$u_\epsilon = V_f + V_b \tag{13}$$

$$u_\rho = V_f - V_b \tag{14}$$

$$\ddot{\epsilon} = b_1 u_\epsilon + D_\epsilon \tag{15}$$

$$\dot{x}_2 = x_3 + b_1 u_\epsilon \tag{16}$$

$$\dot{x}_3 = h \approx 0 \tag{17}$$

$$\begin{bmatrix} \dot{x}_1 \\ \dot{x}_2 \\ \dot{x}_3 \end{bmatrix} = \begin{bmatrix} x_2 \\ x_3 \\ h \end{bmatrix} + \begin{bmatrix} 0 \\ b_1 \\ 0 \end{bmatrix} \cdot u_\epsilon \tag{18}$$

$$\begin{bmatrix} \dot{\hat{x}}_1 \\ \dot{\hat{x}}_2 \\ \dot{\hat{x}}_3 \end{bmatrix} = \begin{bmatrix} \hat{x}_2 \\ \hat{x}_3 \\ 0 \end{bmatrix} + \begin{bmatrix} 0 \\ b_1 \\ 0 \end{bmatrix} \cdot u_\epsilon + L_\epsilon \cdot (x_1 - \hat{x}_1) \tag{19}$$

$$L_\epsilon = [3\omega_{0\epsilon} \ 3\omega_{0\epsilon}^2 \ \omega_{0\epsilon}^3] \tag{20}$$

$$\ddot{\rho} = b_2 u_\rho + D_\rho \tag{21}$$

$$\dot{x}_5 = x_6 + b_2 u_\rho \tag{22}$$

$$\dot{x}_6 = h \approx 0 \tag{23}$$

$$\begin{bmatrix} \dot{x}_4 \\ \dot{x}_5 \\ \dot{x}_6 \end{bmatrix} = \begin{bmatrix} x_5 \\ x_6 \\ h \end{bmatrix} + \begin{bmatrix} 0 \\ b_2 \\ 0 \end{bmatrix} \cdot u_\rho \tag{24}$$

$$\begin{bmatrix} \dot{\hat{x}}_4 \\ \dot{\hat{x}}_5 \\ \dot{\hat{x}}_6 \end{bmatrix} = \begin{bmatrix} \hat{x}_5 \\ \hat{x}_6 \\ 0 \end{bmatrix} + \begin{bmatrix} 0 \\ b_2 \\ 0 \end{bmatrix} \cdot u_\rho + L_\rho \cdot (x_4 - \hat{x}_4) \tag{25}$$

$$L_\rho = [3\omega_{0\rho} \ 3\omega_{0\rho}^2 \ \omega_{0\rho}^3] \tag{26}$$

Now we can reach the voltage inputs of the front and back motors as below equations (27) and (28). On the other hand, the pitch reference is produced by employing a classic PID controller through the travel reference and applied to the plant dynamics.

$$V_f = \frac{u_\epsilon + u_\rho}{2}, \quad V_b = \frac{u_\epsilon - u_\rho}{2} \tag{27} \tag{28}$$

3.2. Fuzzy Logic Controller

In order to design this type of controller on the elevation and pitch dynamics, first we should define subjectively, what is negative high (NH), negative low (NL), zero (Z), positive low (PL), positive high (PH) on the angles and angle speeds. In the first case, the range of the triangle membership functions of the fuzzy sets are defined as table 1, and then they are specified in a narrower range as table 2. Now several rules are dedicated that determine what the output in certain situations is. Number of rules for each of elevation and pitch controllers will be 25. Table 3 demonstrates these rules, which gives range of front and back motor voltage level as the controller output, based on the range of angles and their speeds. Schematic of an FLC controller for the motions dynamics is shown in figure 3.

TABLE 1

RANGE OF THE ELEVATION, PITCH AND THEIR SPEEDS IN THE FIRST CASE

	NH	NL	Z	PL	PH
ϵ	-45 / -15	-30 / 0	-15 / +15	0 / +30	+15 / +45
ρ	-90 / -30	-60 / 0	-30 / +30	0 / +60	+30 / +90
$\dot{\epsilon}$	-90 / -30	-60 / 0	-30 / +30	0 / +60	+30 / +90
$\dot{\rho}$	-90 / -30	-60 / 0	-30 / +30	0 / +60	+30 / +90
u_ϵ	-810 / -270	-540 / 0	-270 / +270	0 / +540	+270 / +810
u_ρ	-90 / -30	-60 / 0	-30 / +30	0 / +60	+30 / +90

TABLE 2

RANGE OF THE ELEVATION, PITCH AND THEIR SPEEDS IN THE SECOND CASE

	NH	NL	Z	PL	PH
ϵ	-30 / -10	-20 / 0	-10 / +10	0 / +20	+10 / +30
ρ	-45 / -15	-30 / 0	-15 / +15	0 / +30	+15 / +45
$\dot{\epsilon}$	-45 / -15	-30 / 0	-15 / +15	0 / +30	+15 / +45
$\dot{\rho}$	-45 / -15	-30 / 0	-15 / +15	0 / +30	+15 / +45
u_ϵ	-810 / -270	-540 / 0	-270 / +270	0 / +540	+270 / +810
u_ρ	-90 / -30	-60 / 0	-30 / +30	0 / +60	+30 / +90

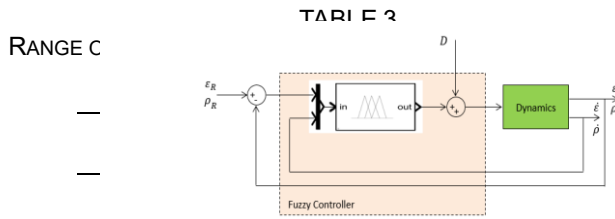


Fig. 3. Schematic of Fuzzy Logic Controller

PL	PL	Z	NL	NH	NH
PH	Z	NL	NH	NH	NH

3.3. Back Stepping Controller

This type of controller is useful when there are state dependency in the motion dynamics [13]. The main objective is to design a controller ensuring that the elevation, pitch and travel motions track the desired reference values asymptotically. The *Lyapunov* stability theory forms the basis of this control methodology. This theorem shows that any positive definite matrix Q like an identity matrix can be used to determine the stability of a linear system. Based on the described theorem 3.6 in the reference book [16], P matrix can be derived as the equation (29). Based on the state vector definition presented in equation (30), the corresponding P matrix in our dynamics will be as equation (31), which is positive definite, and therefore our control system can be globally asymptotically stable.

$$P = A^T Q + Q A \quad (29)$$

$$X = [x_1 \ x_2 \ x_3 \ x_4 \ x_5 \ x_6 \ x_7 \ x_8] = [\varepsilon \ \rho \ \lambda \ \dot{\varepsilon} \ \dot{\rho} \ \dot{\lambda} \ \int R_\varepsilon - \varepsilon \ \int R_\rho - \rho] \quad (30)$$

$$P = \begin{bmatrix} 0 & 0 & 0 & 1 & 0 & 0 & 1 & 0 \\ 0 & 0 & 0 & 0 & 1 & b_1 & 0 & 1 \\ 0 & 0 & 0 & 0 & 0 & 1 & 0 & 0 \\ 1 & 0 & 0 & 0 & 0 & 0 & 0 & 0 \\ 0 & 1 & 0 & 0 & 0 & 0 & 0 & 0 \\ 0 & b_1 & 1 & 0 & 0 & 0 & 0 & 0 \\ 1 & 0 & 0 & 0 & 0 & 0 & 0 & 0 \\ 0 & 1 & 0 & 0 & 0 & 0 & 0 & 0 \end{bmatrix} \quad (31)$$

In order to design this controller for elevation and pitch motion dynamics and extract the corresponding control inputs, the below described procedure is implemented. We start with the elevation dynamics.

$$\dot{x}_1 = x_4 \quad (32)$$

$$\dot{x}_4 = b_1 u_\varepsilon \quad (33)$$

$$e_1 = R_\varepsilon - \varepsilon \rightarrow \dot{e}_1 = \dot{R}_\varepsilon - \dot{\varepsilon} - x_4 \quad (34)$$

If x_4 were the control input, by selecting $x_4 = c_1 e_1 + \dot{R}_\varepsilon$ we

will have $\dot{e}_1 = -c_1 e_1$ and it guaranties exponential convergence of the error to zero. Here c_1 determines how fast the error converges to zero. Now, let consider the reference value for x_4 be as the equation (35), as if it were a virtual control input, where c_1 and α_1 are positive constants.

$$R_{x_4} = c_1 e_1 + \dot{R}_\varepsilon + \alpha_1 E_1, \quad E_1 = \int_0^t e_1(\tau) d\tau \quad (35)$$

$$e_2 = R_{x_4} - x_4 = c_1 e_1 + \dot{R}_\varepsilon + \alpha_1 E_1 - x_4 \quad (36)$$

$$\rightarrow x_4 = c_1 e_1 + \dot{R}_\varepsilon + \alpha_1 E_1 - e_2 \quad (37)$$

$$\dot{e}_1 = \dot{R}_\varepsilon - \dot{x}_4 \rightarrow \dot{e}_1 = -c_1 e_1 - \alpha_1 E_1 + e_2 \quad (38)$$

$$e_2 = R_{x_4} - \dot{x}_4 = c_1 \dot{e}_1 + \dot{R}_\varepsilon + \alpha_1 \dot{e}_1 - \dot{x}_4 \quad (39)$$

$$\rightarrow \dot{e}_2 = c_1(-c_1 e_1 - \alpha_1 E_1 + e_2) + \ddot{R}_\varepsilon + \alpha_1 \dot{e}_1 - \dot{x}_4 \quad (40)$$

Let the desired dynamics for e_2 is given as $\dot{e}_2 = -c_2 e_2 - e_1$, where c_2 is a positive constant, so we will have:

$$\dot{e}_2 = -c_2 e_2 - e_1 = c_1(-c_1 e_1 - \alpha_1 E_1 + e_2) + \ddot{R}_\varepsilon + \alpha_1 \dot{e}_1 - b_1 u_\varepsilon \quad (41)$$

So we can consider u_ρ as the control inputs of the pitch dynamics as:

$$(1 + \alpha_1 - c_1^2)e_1 + (c_1 + c_2)e_2 - c_1 \alpha_1 E_1 + \ddot{R}_\varepsilon = b_1 u_\varepsilon$$

$$u_\varepsilon = \frac{(1 + \alpha_1 - c_1^2)e_1 + (c_1 + c_2)e_2 - c_1 \alpha_1 E_1 + \ddot{R}_\varepsilon}{b_1} \quad (42)$$

Similarly we can implement the same procedure for extracting u_ρ as the control input of the pitch dynamics as below.

$$u_\rho = \frac{(1 + \alpha_2 - c_3^2)e_3 + (c_3 + c_4)e_2 - c_3 \alpha_2 E_2 + \ddot{R}_\rho}{b_2} \quad (43)$$

By tuning the positive parameters c_1, c_2, c_3, c_4 the desired performance is expected. As mentioned, these parameters determine how fast $\varepsilon \rightarrow R_\varepsilon$, and $\rho \rightarrow R_\rho$. Similar to the ADRC controller, the voltage level of the front and back motor can be derived as presented in the equations (27) and (28).

4 TEST AND RESULTS

To evaluate the behaviors of three presented control architectures on the elevation and pitch dynamics, the desired references are set as below.

$$R_\varepsilon = 0.2 \text{ rad}, \quad R_\rho = 0.1 \text{ rad} \quad (44)$$

Then the below desired reference is applied on the travel dynamics, to evaluate the control architectures and track the desired path on the elevation and travel motions.

$$R_\lambda = 0.5 \text{ rad} \quad (45)$$

First the behavior of ADRC controller is evaluated. Here by applying a disturbance signal on the elevation and pitch dynamics shown in the figure 4, the controller ability to eliminate it is studied. Figures 5 and 6 display the reference and measured elevation and pitch angles. Despite having disturbance on the dynamics, the measured outputs can successfully track the given reference inputs. It is worth mention that, increasing of the controller bandwidth may conclude more accurate in tracking but it becomes more sensitive to the sensor noise. By applying the desired reference on the travel dynamics, the tracked travel and pitch angles are illustrated in the figures 7 and 8. As a visual result, we can see the designed controller can well track the desired references.

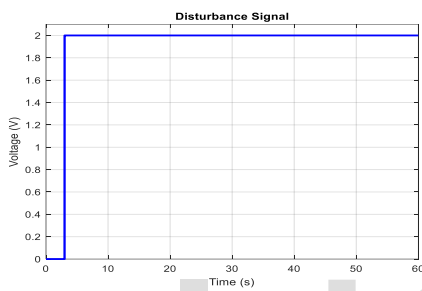


Fig. 4. Applied External Disturbance on the Elevation and Pitch Dynamics

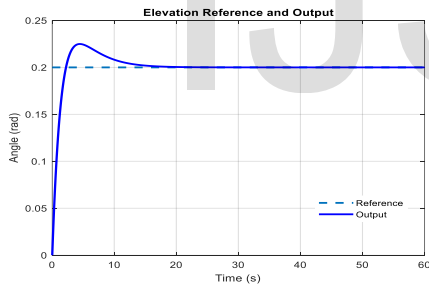


Fig. 5. Elevation Reference and Output by ADRC Controller

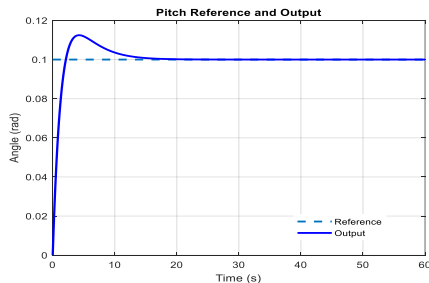


Fig. 6. Pitch Reference and Output by ADRC Controller

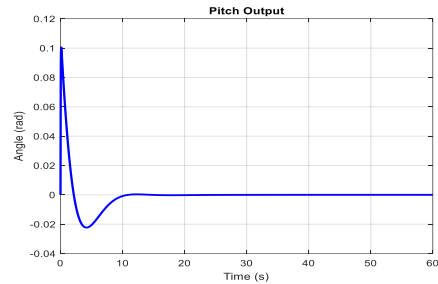
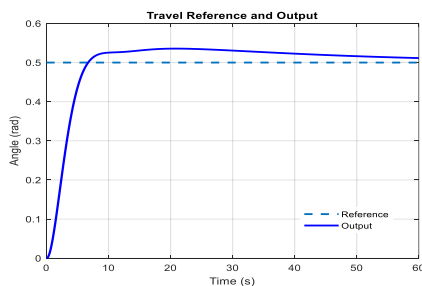


Fig. 8. Pitch Output

Secondly the behavior of FLC controller is evaluated in the mentioned two cases. In the first case, wider range of membership functions, as it is seen from the figures 9 and 10, although the response of pitch motion is acceptable, but the elevation motion response is not satisfactory. In the second case, narrower range of membership functions, the responses are accepted. Figures 11 and 12 display the reference and measured elevation and pitch angles in the second case. Then by applying the desired reference on the travel dynamics, the tracked travel and pitch angles are displayed in the figures 13 and 14. As a visual result, we can see the designed controller can well track the desired references.

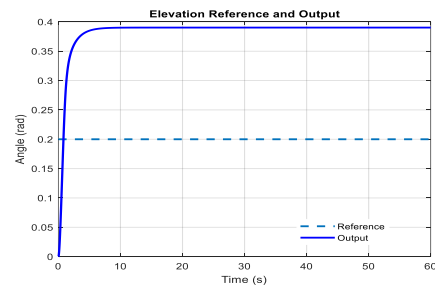


Fig. 9. Elevation Reference and Output by FLC Controller in the First Case

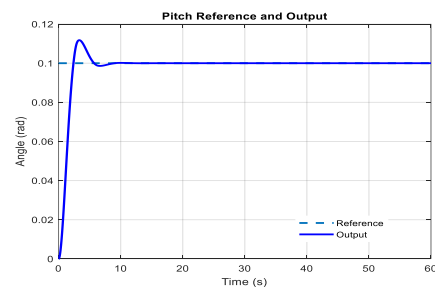


Fig. 10. Pitch Reference and Output by FLC Controller in the First Case

Finally the behavior of BSC controller is evaluated. Figure 15 and 16 show the reference and measured elevation and pitch angles employing this controller. It is worth mentioning that, increasing of the parameters c_1, c_2, c_3, c_4 , concludes less settling times in the responses but they will have more steady state errors. Then by applying the desired reference on the travel dynamics, the tracked travel and pitch angles are displayed in the figures 17 and 18. As a visual result, we can see the designed controller can well track the desired references.

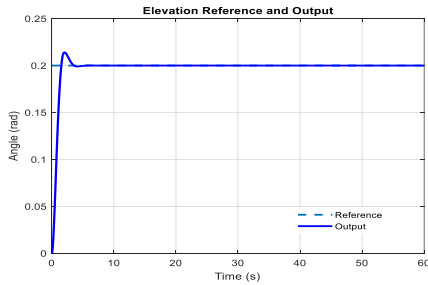


Fig. 11. Elevation Reference and Output by FLC Controller in the Second Case

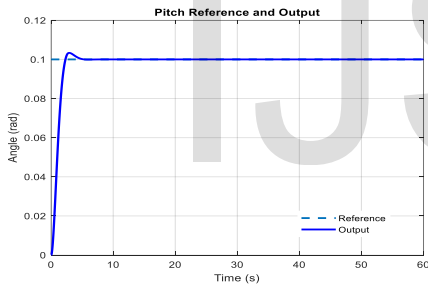


Fig. 12. Pitch Reference and Output by FLC Controller in the Second Case

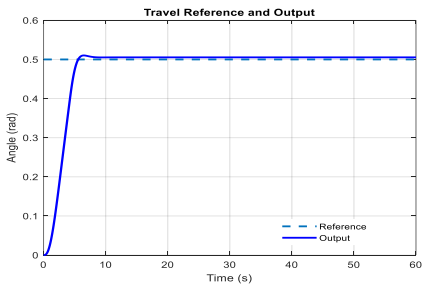


Fig. 13. Travel Reference and Output by FLC Controller

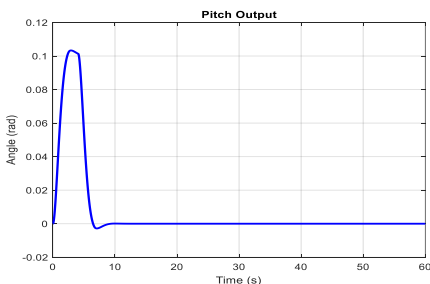


Fig. 14. Pitch Reference and Output by FLC Controller

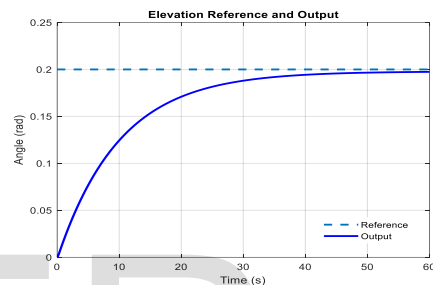


Fig. 15. Elevation Reference and Output by BSC Controller

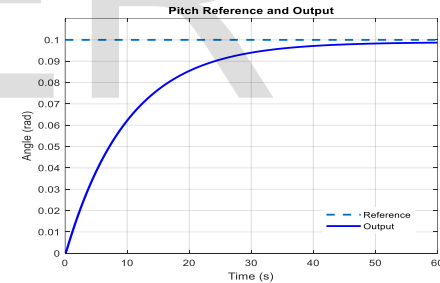


Fig. 16. Pitch Reference and Output by BSC Controller

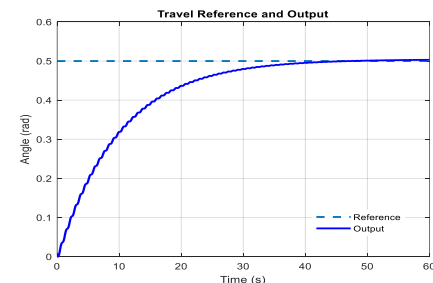


Fig. 17. Travel Reference and Output

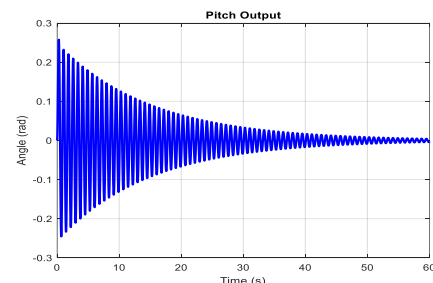


Fig. 18. Pitch Output

In all of designed controllers, we can conclude that the output signals can successfully track the input reference signals. But in order to compare the behavior of the designed controllers more carefully, their performances measures are calculated as displayed in the table 4. Based on these values, we can conclude some notable issues. In the elevation dynamics, ADRC has smaller error energy, FLC gives the nearest response with respect to the applied reference, and has smaller steady-state error, while the BSC has larger error energy, gives the furthest response with respect to the applied reference, and has larger steady-state error. Since in most of cases, the performance measures of the ADRC along with an FLC are smaller than the BSC, it can be concluded that ADRC is more accurate in tracking the reference input of both elevation and pitch dynamics. These preference is realized though annoying applied disturbances.

5 DISCUSSION AND CONCLUSION

In this paper, we have presented designing and implementing of control architectures for a three-DOF helicopter by active disturbance rejection (ADRC), fuzzy logic (FLC) and back-stepping (BSC) controllers in order to drive the helicopter to a desired trajectory. Also a proper extended state observer (ESO) was designed to eliminate the external disturbances effecting on the system. The simulation results show the good performance of three proposed control approaches. In other words, the elevation and pitch angles can successfully track the given reference inputs. The excellent performance of the ADRC comes with elimination of the applied external disturbance on the elevation and pitch dynamics. The performance of three architectures were compared employing the mathematical control measures. It was concluded, the ADRC control along with an FLC is more accurate in tracking the desired reference input.

REFERENCES

[1] Laboratory Guide, 3 DOF Helicopter Experiment for MATLAB/Simulink Users, QUANCER
 [2] Rajappa, Sujit, et al. "Modelling and dynamic identification of 3 DOF Quanser helicopter." *2013 16th International Conference on Advanced Robotics (ICAR)*. IEEE, 2013.

[3] Brentari, Mirko, et al. "Benchmark model of Quanser's 3 DOF Helicopter." (2018).
 [4] Le Gac, Sylvain, Dimitri Peaucelle, and Boris Andrievsky. "Adaptive Parameter Identification for Simplified 3D-Motion Model of 'LAAS Helicopter Benchmark'." *IFAC Proceedings Volumes* 40.13 (2007): 244-249.
 [5] Mariya, A. Ishutkina. "Design and Implementation of a Supervisory Safety Control for 3DOF Helicopter." *Department of Aeronautics and Astronautics* (2004).
 [6] Mansor, Hasmah, et al. "Performance comparisons between PID and adaptive PID controllers for travel angle control of a bench-top helicopter." *Int J Electr Comput Electron Commun Eng* 9.1 (2015): 35-40.
 [7] Brantner, Gerald, et al. "A detailed nonlinear dynamic model of a 3-DOF laboratory helicopter for control design." *IFAC Proceedings Volumes* 45.2 (2012): 216-221.
 [8] J. Witt, S. Sudchai and H. Werner, "Approximate Model Predictive Control of a 3-DOF Helicopter", *Proceeding of the 46th IEEE Conference on Design and Control*, Dec. 12-14, 2007, New Orleans, LA, USA.
 [9] F. Zhou, D. Li, P. Xia, "Research of Fuzzy Control for Elevation Attitude of 3-DOF Helicopter", *International Conference on Intelligent Human-machine Systems and Cybernetics*, 2009, Beijing University, China.
 [10] H. Rios, A. Rosales, A. Ferreira and A. Davila, "Robust Regulation for a 3-DOF Helicopter via Sliding-Mode Control and Observation Techniques", *American Control Conference*, June 30-July 02, 2010, Marriott Waterfront Baltimore, MD, USA.
 [11] Z. Liu, Z. Choukri and H. Shi, "Control Strategy design Based on Fuzzy Logic and LQR for 3-DOF helicopter Model", *International Conference on Intelligent Control and Information Processing*, August 13-15, 2010, Dalian, China.
 [12] H. Liu, G. Lu and Y. Zhong, "Robust LQR attitude Control of a 3-DOF Laboratory Helicopter for Aggressive Maneuvers", *IEEE Transactions on Industrial Electronics*, Vol 60, No. 10, October 2013.
 [13] Zheng Fang, Weinan Gao and Lei Zhang, "Robust Adaptive Integral Backstepping Control of a 3-DOF Helicopter", *International Journal of Advanced Robotic Systems*, May 2012, Northeastern University, China.
 [14] Sadeghi, Amir Noabahr, Kutluk Bilge Arkan, and Mehmet Efe Özbek. "Torsional model of the drill string, and real-time prediction of the bit rotational speed and the torque on bit, in an oil well drilling tower." *Journal of Petroleum Science and Engineering* (2020): 107814.
 [15] Gao, Zhiqiang. "Scaling and bandwidth- parameterization based controller tuning." *Proceedings of the American control conference*. Vol. 6. 2006.

TABLE 4
 PERFORMANCE MEASURES OF THE CONTROLLERS OF THE ELEVATION AND PITCH ANGLES

Error Measure	ADRC Elevation	ADRC Pitch	FLC Elevation	FLC Pitch	BSC Elevation	BSC Pitch
ISE	2.18	0.52	2.24	0.73	20.83	25.21
IAE	32.38	15.46	17.13	10.93	211.82	105.91
ITAE	124.59	56.82	11.42	8.58	2336.20	1168.10
RMSE	0.42	0.20	0.22	0.14	2.73	1.37

[15] J.Jacques and E.Slotine , "*Applied Nonlinear Control*", Book.

IJSER